Journal of Optoelectronics and Advanced Materials Vol. 7, No. 1, February 2005, p. 161 - 168

Invited Paper

SUB-BANDGAP ABSORPTION SPECTROSCOPY AND MINORITY CARRIER TRANSPORT PROPERTIES OF HYDROGENATED MICROCRYSTALLINE SILICON THIN FILMS

M. Güneş*, O. Göktaş, S. Okur, N. Işık, R. Carius[a], J. Klomfass[a], F. Finger[a]

Department of Physics, Izmir Institute of Technology, Gülbahçe Kampus 35430 Urla-Izmir, Turkey
[a]Institut für Photovoltaik, Forschungszentrum Jülich, GmbH, 52425 Jülich, Germany

Hydrogenated microcrystalline silicon thin films have been prepared using HW-CVD and VHF-PECVD techniques with different silane concentrations. The steady-state photoconductivity, dual beam photoconductivity, photothermal deflection spectroscopy and steady-state photocarrier grating (SSPG) methods have been used to investigate the optical and electronic properties of the films. Two different sub-bandgap absorption methods have been applied and analyzed to obtain a better insight into the electronic states involved. For some films, differences existed in the optical absorption spectra when the measurements were carried out through the film side and through the substrate side. In addition, for some films, fringe patterns remained on the spectrum after the calculation of the fringe free absorption spectrum, which indicates that structural inhomogeneities were present throughout the film. Finally, minority carrier diffusion lengths deduced from the SSPG measurements were investigated as a function of the crystalline volume fraction (I_c^{RS}) obtained from Raman spectroscopy. The longest diffusion lengths and lowest sub-bandgap absorption coefficients were obtained for films deposited in the region of the transition to the amorphous growth.

(Received December 9, 2004; accepted January 26, 2005)

Keywords: Hydrogenated microcrystalline silicon, Sub-bandgap absorption, Steady-state photocarrier grating, Dual beam photoconductivity

1. Introduction

Hydrogenated microcrystalline silicon (μc-Si:H) thin films have become an important candidate for large area photovoltaic applications [1,2]. Thin films prepared by very high frequency plasma enhanced chemical vapour deposition (VHF-PECVD) already exhibit excellent quality and performance in photovoltaic devices [1,2]. Similarly, much progress has been made in the preparation of thin films and solar cells using the hot-wire chemical vapour deposition (HW-CVD) technique [3,4]. An intrinsic characteristic of μc-Si:H is its microstructure, which is mainly controlled by varying the silane concentration, SC, (gas flow ratio [SiH4]/[SiH4 + H2]) during deposition. An important property of μc-Si:H thin films is the optical absorption coefficient, α(hν), spectrum, especially at sub-bandgap energies. Well established methods such as photothermal deflection spectroscopy (PDS) [5] and transmission and reflection (T&R) spectroscopy [6] have been extensively used to measure the α(hν) spectrum. It is generally accepted that both methods have limitations at lower energies in obtaining reliable absorption coefficients for the bulk material. Alternatively, photoconductivity techniques such as the constant photocurrent method (CPM), both in standard [7] and absolute mode [8] and the dual beam photoconductivity (DBP) [9] method have

*Corresponding author: mehmetgunes@iyte.edu.tr

been used to derive absorption coefficients from the measured photoconductivity spectrum. In the absolute CPM mode, the absorptance over transmittance (A/T) spectrum has been used to calculate the $\alpha(h\nu)$ spectrum using the Ritter-Weiser formula [10]. In the DBP method, the DBP yield spectrum is normalized to the absolute $\alpha(h\nu)$ obtained from the T&R, after removal of interference fringes from the spectrum. For films less than 1 μm thick, significant errors can be introduced in the shape and magnitude of the spectrum due to large interference fringes, when a fast Fourier transform process [11] is used for fringe removal. Furthermore, T&R measurements are unable to provide accurate absorption coefficients at normalization energies for such thin films. To overcome these difficulties, a novel approach was introduced to obtain a reliable normalization of the relative fast Fourier transformed fringe free DBP yield spectrum [12]. This involves a tedious detailed analysis of the dielectric functions and known densities of extended states. However, no study has yet been reported for the direct calculation of the fringe-free absolute $\alpha(h\nu)$ spectrum from the relative DBP yield spectrum. In the present work, the DBP yield spectrum and simultaneously measured transmission signal have been used to calculate the fringe-free $\alpha(h\nu)$ spectrum of μc-Si:H films deposited with different SCs using the VHF-PECVD and HW-CVD methods. It is compared with the $\alpha(h\nu)$ spectrum measured independently by PDS on the same μc-Si:H films. In addition, ambipolar diffusion lengths were measured using the steady-state photocarrier grating (SSPG) method [13], to understand the effects of microstructure on the minority carrier properties.

2. Experimental details

Device quality intrinsic hydrogenated microcrystalline silicon thin films were prepared using a multichamber deposition system with three PECVD chambers and one HW-CVD chamber, at the Research Center Juelich. They were deposited on borosilicate glass substrates with varying silane concentrations from 2 to 7% [2-4] at substrate temperatures between 185 and 220°C. The film thickness varied between 0.4 and 0.80 μm, and the metal contacts were 0.5 mm wide and 0.5 cm long. Steady-state photoconductivity (SSPC) measurements were carried out using 800 and 750 nm interference filters, together with a calibrated ENH-type white light source. The applied dc bias was in the Ohmic region of the contacts. A standard PDS system [5] was used to measure the raw PDS spectrum, and the transmission signal was simultaneously measured from the substrate side of the sample. A detailed description of the DBP method applied to μc-Si:H films can be found elsewhere [14]. Here DBP measurements were carried out for different dc bias light intensities for both ac light illumination through the film and from the substrate side. The Corresponding transmission spectra were measured from the substrate and film sides. Interference fringe-free absolute $\alpha(h\nu)$ spectra were calculated from both the PDS and the DBP spectra, using a procedure [15] based on the Ritter-Weiser formula [10]. Ambipolar diffusion lengths were measured using a standard SSPG technique [13]. A polarized He-Ne laser of wavelength 633 nm was used to measure the photocurrent ratio, β, for different grating periods, Λ, at constant dc bias voltages for which the β values were independent of the applied electric field. The I_c^{RS} values were obtained from Raman measurements [2,3] carried out on the same samples.

3. Results and discussion

Intrinsic μc-Si:H thin films prepared using the VHF-PECVD method already show excellent photoconductive properties [1,2]. The $\mu_n\tau_n$-products for majority carrier electrons versus the generation rate obtained from SSPC measurements are shown in Figure 1 for intrinsic μc-Si:H thin films deposited by VHF-PECVD and hot-wire CVD, for varying silane concentrations (SC). The $\mu_n\tau_n$-products show a characteristic dependence on the generation rate, G, and decrease as G increases with the exponent (γ-1). The parameter γ has similar values for both types of film, and changes from 0.8 to 1.0 indicating a continuous distribution of recombination centers present in these structurally inhomogeneous materials. However, for samples deposited with SCs from 3.7 to

7%, VHF-PECVD films have values almost a factor of ten higher than those of HW-CVD films. For a highly crystalline sample prepared by HWCVD with SC = 2.5%, the $\mu_n\tau_n$-products degraded substantially to a value of 10^{-8} cm^2/V, due to the increased density of defect states [16] present in the sample.

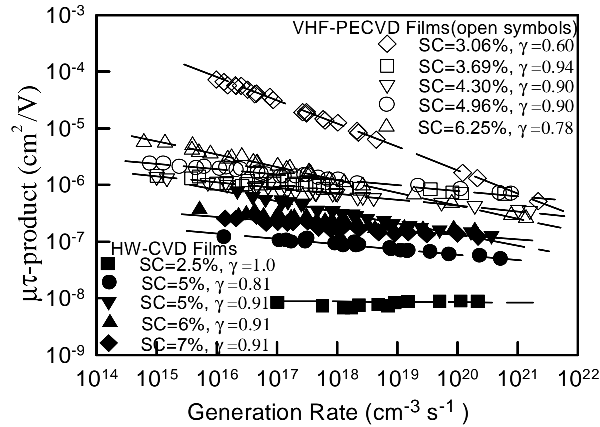

Fig. 1. Mobility.lifetime products versus generation rate for intrinsic μc-Si:H films deposited using VHF-PECVD and HW-CVD, for different SCs.

To investigate the effects of these defect states, sub-bandgap absorption methods have been used extensively to compare thin films prepared under different deposition conditions. In this work, PDS and DBP methods were independently used to obtain the absorption coefficient spectra of intrinsic μc-Si:H thin films, in a wider energy range. In Figure 2a, typical results of the raw PDS and DBP yield spectra, Y_{DBP}, measured for two different dc bias light intensities are shown for an intrinsic μc-Si:H film prepared by VHF-PECVD with SC = 4.3%. Corresponding transmission signals for these two methods are illustrated in Figure 2b. By using the raw PDS spectrum, a rough calculation of the absolute absorption coefficient spectrum can be carried out, as described elsewhere [5]. In this work, an interference fringe-free $\alpha(h\nu)$ spectrum was calculated from the raw PDS spectrum and the simultaneously measured transmission signal shown in Figure 2b, using a procedure [15] based on the Ritter-Weiser formula [10]. The calculated absolute $\alpha(h\nu)$ spectrum at sub-bandgap energies is very high, as shown in Fig. 3 by the open square symbols. This is

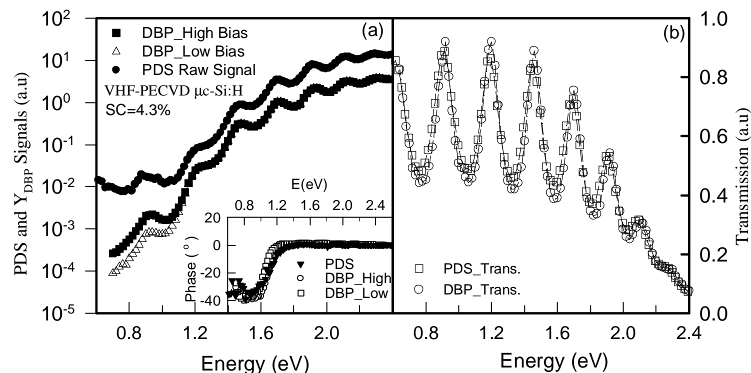

Fig. 2. (a) Raw PDS and DBP Yield spectra of a μc-Si:H thin film deposited by VHF-PECVD with SC = 4.3%. The inset shows the phase of the PDS and DBP measurements. (b) Simultaneously measured corresponding transmission signals for the PDS and DBP methods.

attributed to the absorption of the substrate and the highly defective surface layer. This effect can also be seen from the phase of the PDS as given in the inset of Figure 2, where the phase changes below 1.2 eV are due to substrate absorption. Using the changes in the phase of the PDS, a phase correction to the PDS spectrum is carried out and the effects of substrate and surface absorption are eliminated from the α(hν) spectrum. The α(hν) values at sub-bandgap energies for the phase corrected PDS (filled squares) decreased substantially, as seen from Figure 3. However, the accuracy of the phase correction procedure was not better than factor of two due to noise in the phase signal.

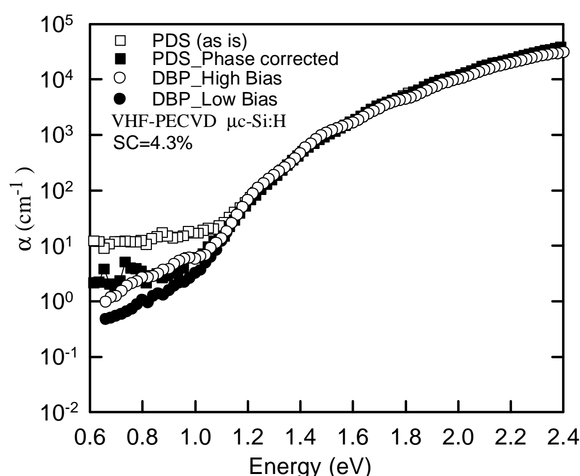

Fig. 3. Absolute absorption coefficient spectra of a μc-Si:H thin film deposited by the VHF-PECVD method with SC = 4.3%, independently obtained from PDS and DBP measurements.

Alternatively, we have used the DBP method to measure a relative DBP yield spectrum, Y_{DBP}, as shown in Figure 2. The shape of Y_{DBP} is similar to the raw PDS spectrum, and the transmission signals are identical for the same sample. When the required conditions are satisfied, Y_{DBP} becomes proportional to the absorbance. In this work, for the first time, Y_{DBP} and the simultaneously measured transmission signal were used to calculate the absolute α(hν) spectrum, without carrying out any normalization procedure to the PDS or to the T&R as commonly practiced in the literature, using the same procedure as that applied for the analysis of the PDS spectrum. The α(hν) spectra calculated from DBP for high and low bias light intensities are shown in Figure 3 for the same sample. It is seen that there is a good overlap in the α(hν) spectra, independently obtained from the PDS and DBP measurements at energies, above 1.1 eV. However, differences exist below the bandgap energy. The α(hν) values of DBP spectrum in the sub-bandgap region show not the absolute absorption coefficient but the effects of the occupied defect states present in the bandgap, which can be easily modified by the intensity of the dc bias light. For low bias light conditions, DBP probes a distribution of occupied defect states very close to that in the dark, i.e. the distribution probed by the constant photocurrent method (CPM). When the intensity of the bias light is increased, the density of electron-occupied defect states above the Fermi level increases as the quasi-Fermi levels move closer to the respective band edges. This results in an increase in the number of transitions from the occupied defect states to the conduction band at sub-bandgap energies. As a result, the α(hν) values at sub-bandgap energies show an increase in the spectrum, which is mainly determined by the nature, density and energy location of the defect states present in the bandgap.

The effects of the occupied defect states are also reflected in the phase of the DBP signal, as shown in the inset of Fig. 2. The large phase change below 1.2 eV indicates that defect kinetics different from that for the extended states is involved in the DBP measurements. The phase of the DBP below 2.0 eV also shows small modulations due to the inhomogeneous photoresponse of the material. This results in a very small fringe pattern left in the calculated α(hν) spectrum below 2.0

eV, as seen in Fig. 3. Similarly, DBP yield spectra of other μc-Si:H films deposited by the VHF-PECVD method with SC = 3.06 to 6.25% have been measured for two different bias light intensities. The corresponding absolute α(hν) spectra have been calculated, and compared with those independently measured by PDS (data not shown). It was found that there is a good overlap in the α(hν) spectra at energies above the bandgap energy. However, at sub-bandgap energies, the α(hν) values obtained from the low bias light DBP measurement are always lower than those of the phase corrected PDS spectrum.

Similar quality intrinsic μc-Si:H thin films have also been deposited using HW-CVD for the same range of SCs, which results in different crystalline to amorphous volume fractions in the microstructure. The effects of the changes in microstructure on the α(hν) spectrum were also investigated using the same methods. In this case, DBP measurements were carried out by illuminating ac light through film side and through the substrate side, using the same intensity as for the dc bias case. The DBP yield spectra of an intrinsic μc-Si:H film prepared by HW-CVD with SC = 4% are shown in Figure 4a for front and back ac illuminations. For front ac illumination, Y_{DBP} measured at high and low bias light intensities shows a consistent difference at lower energies, as in the case of the VHF-PECVD sample of Figure 2. However, the shape of Y_{DBP} measured using back ac illumination is different from that of front ac illumination, where the peaks of the interference fringes are shifted to higher energy. The resulting α(hν) spectra calculated using the corresponding transmission signals shown in the inset are illustrated in Figure 4b, together with that of PDS. Here, the PDS data are not corrected for substrate absorption due to the large scatter in the phase of the PDS signal. It is clearly seen that there is very good overlap in the spectra of PDS and DBP front ac illumination above the bandgap energy, as observed for VHF-PECVD films. For sub-bandgap energies, lower α(hν) values were obtained using the DBP low bias light intensity measurement. Contrastingly, the α(hν) spectrum for DBP back ac illumination measured at the same high bias light intensity was completely different from that for the corresponding DBP front ac illumination, even though the transmission signals of these measurements were almost identical. There remain interference fringes with a large modulation depth after fringe-free calculation of the α(hν) spectrum. It can be inferred that there exists a defective interfacial layer at the film-substrate interface, which causes high levels of recombination and a decrease in the photoresponse. This kind of severe change in the DBP spectrum as ac light is illuminated through the substrate side was not seen systematically in other intrinsic samples.

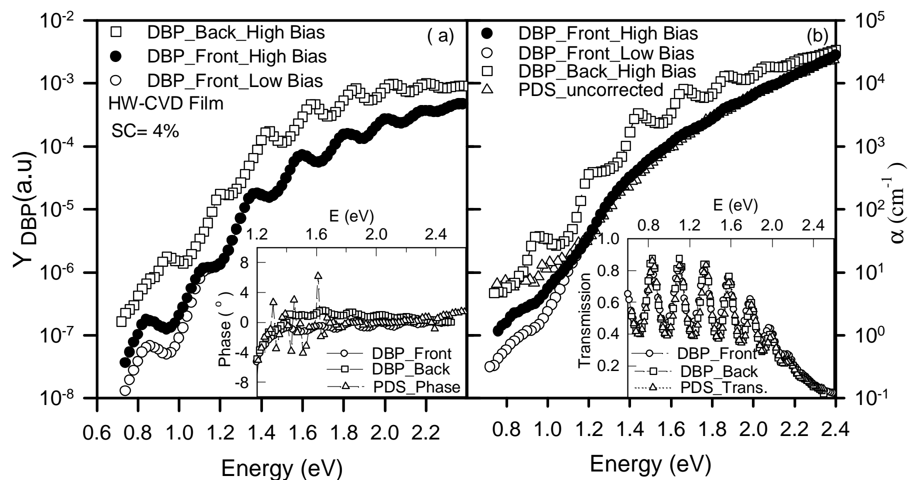

Fig. 4. (a) DBP yield spectra of a μc-Si:H thin film deposited by HW-CVD for front ac illumination and back ac illumination, which is shifted vertically for clarity. In the inset, the phase of the DBP signals and that of PDS are shown. (b) Calculated absorption coefficient spectra of DBP measurements for both front and back ac illuminations and that of PDS independently measured on the same sample. The inset shows corresponding transmission signals for DBP front and back ac illuminations and that of PDS.

In order to investigate the effects of changes in the microstructure on the α(hν) spectrum at sub-bandgap energies, the results of phase corrected PDS and low bias light DBP measurement with front ac illumination will be used for comparing different samples.

As a summary of the sub-bandgap absorption results, the effects of the changes in microstructure on the α(hν) values at 0.8 eV are shown in Figures 5a and 5b, for intrinsic μc-Si:H thin films deposited by HW-CVD and VHF-PECVD respectively. In order to represent the changes in microstructure, the crystalline volume fraction I_c^{RS} values are used instead of the silane concentration (SC). This allows us to compare different samples prepared under slightly different deposition conditions. For both types of intrinsic film, the α(0.8eV) values measured by low bias light DBP are lower than those obtained from the phase corrected PDS measurements.

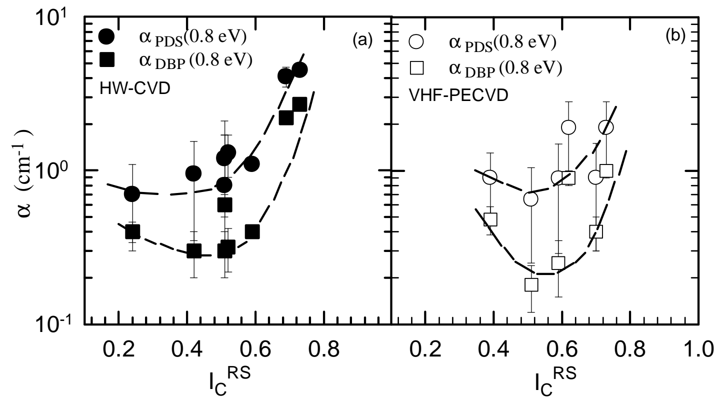

Fig. 5. The α(0.8eV) values from PDS and low bias light DBP front ac illumination versus I_c^{RS} for intrinsic μc-Si:H thin films deposited by (a) HW-CVD and (b) VHF-PECVD. The broken lines are guides to the eye.

There exists approximately a factor of two difference between the PDS and DBP curves. Both curves show a decrease as I_c^{RS} decreases. The lowest α(0.8eV) value occurs at around 0.5 for both HW-CVD and VHF-PECVD films, then it tends to increase for lower I_c^{RS} values. The results in Fig. 5 indicate that intrinsic μc-Si:H thin films deposited in the transition region have the lowest defect density, and will provide better performances when solar cells are fabricated using these materials as the absorber layers. This has already been confirmed by studies reported in the literature for both VHF-PECVD [1, 2] and HW-CVD materials [3,4,19].

Apart from the effects of the microstructure on the sub-bandgap absorption coefficient, correlations between the structural and the minority carrier transport properties are also important in improving the efficiency of solar cells made from these materials. In Figure 6, the ambipolar diffusion length, L_{amb}, for minority carrier holes measured using the SSPG method are shown, as a function of the crystalline volume fraction, I_c^{RS} for both VHF-PECVD and HW-CVD films. For pure amorphous films (a-Si:H), L_{amb} is around 100 nm. It increases as I_c^{RS} increases and peaks at around 250 nm for a value of I_c^{RS} around 0.5. This condition corresponds to the microcrystalline growth region close to the transition to the amorphous growth region. As I_c^{RS} increases further, highly crystalline films are grown. However, the L_{amb} values decrease sharply due to the increased density of defect states in the material [16]. This is also consistent with the α(0.8eV) values for both types of film, measured by PDS and low bias light DBP as shown in Fig. 5. This can be attributed to the increased density of recombination centers acting for both electrons and holes. It is also interesting to note that the L_{amb} values and corresponding $\mu_p.\tau_p$ products for holes in the transition region are higher for HW-CVD films than for VHF-PECV ones, even though the latter exhibited higher majority carrier electron $\mu_n.\tau_n$ products, as shown in Figure 1. It can be inferred from the low bias light DBP and SSPG results that solar cells fabricated from intrinsic μc-Si:H films at the transition to the amorphous growth region will result in the highest conversion efficiencies. This observation is

consistent with recently reported studies for solar cells deposited using the VHF-PECVD [1, 2, 18] and HW-CVD methods [19].

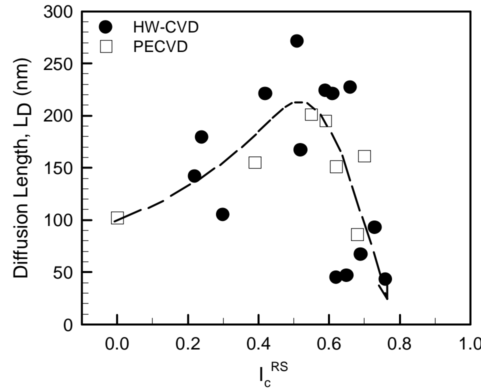

Fig. 6. Diffusion length versus crystalline volume fraction (I_c^{RS}) for intrinsic μc-Si:H thin films deposited using the VHF-PECVD and HW-CVD methods.

4. Conclusions

The electronic and optical properties of intrinsic μc-Si:H thin films deposited using both VHF-PECVD and HW-CVD with the same range of SCs have been investigated using the SSPC, SSPG, PDS, and DBP methods. It has been found that VHF-PECVD films exhibit better majority carrier $\mu_n.\tau_n$ products. However, the effects of the dark Fermi level on these measurements due to oxygen in-diffusion into the microstructure of different types of μc-Si:H films [20] have not been taken into account. The longest L_{amb} is obtained for films prepared in the region of the transition to amorphous growth, for both VHF-PECVD and HW-CVD films. For the first time, the absolute absorption coefficient spectrum was calculated from the relative DBP yield spectrum and the simultaneously measured transmission signal, and the results were compared with the α(hν) spectra independently measured by PDS. A good overlap in the spectra above 1.1 eV was obtained for most of the samples.

For some samples, a fringe pattern remained on the α(hν) spectrum after the fringe free calculation procedure, due to structural inhomogeneities present in the films. Differences existed in the α(hν) spectra of PDS and DBP front ac illumination in the sub-bandgap region. These were approximately a factor of two for all the samples. The systematic difference between the two methods is consistent, since the PDS method detects all transitions from occupied states into empty states when light photons are absorbed. However, the low bias light DBP measurement can only detect the free electrons in the conduction band due to transitions from the occupied defect states into the empty conduction band extended states, not those transitions into states above the Fermi level. For high bias light DBP, an understanding of the α(hν) spectrum is also informative, since the occupation statistics of defect states in the bandgap is substantially changed from the dark condition, which involves the detailed defect generation-recombination kinetics, and the nature, density, and energy location of the defect states. Its analysis will be performed in future research.

The effect of the microstructure characterized by I_c^{RS} on α(0.8eV) is similar for both VHF-PECVD and HW-CVD films. The α(0.8eV) value shows a minimum at around 0.5 for both HW-CVD and VHF-PECVD films, indicating that the lowest defect density films are produced in the region of transition to amorphous growth. These results are also consistent with the L_{amb} values obtained from SSPG measurements carried out on the same samples. However, more investigation is necessary to fully understand the effect of the inhomogeneous microstructure and the effect of instabilities due to in-diffusion of atmospheric gases on the electronic and optical properties of intrinsic μc-Si:H thin films.

Acknowledgements

The authors thank S. Klein, A. Gross, M. Hülsbeck, A. Lambertz, and J. Wolff for helping with sample preparation and measurements. This work is partially supported by the International Bureau of the BMBF, Germany under project number 42.4.I3B.2.A and the Scientific and Technical Research Council of Turkey (TÜBİTAK) under project number TBAG-U/14.

References

[1] A. Shah, E. Vallat-Sauvain, P. Torres, J. Meier, U. Kroll, C. Hof, C. Droz, M. Goerlitzer, N. Wyrsch, M. Vanacek, Mater. Sci. Eng. B **69/70**, 219 (2000).
[2] O. Vetterl, F. Finger, R. Carius, P. Hapke, L. Houben , O. Kluth, A. Lambertz, A. Mück, B. Rech, H. Wagner, Solar Energy Materials Solar Cells **62**, 97 (2000).
[3] S. Klein, F. Finger, R. Carius, T. Dylla, B. Rech, M. Grimm, L, Houben, M. Stutzmann, Thin Solid Films **430**, 202 (2003).
[4] S. Klein, J. Wolff, F. Finger, R. Carius, H. Wagner, M. Stutzmann, Jpn. J. Appl. Phys. **41**, L10 (2002)
[5] W. B. Jackson, N. M. Amer, Phys. Rev. B **25**, 5559 (1982).
[6] G. D. Cody, C. R. Wronski, B. Abeles, R. B. Stephens, B. Brooks, Solar Cells **2** 227 (1980).
[7] M. Vanacek, J. Kocka, J. Stuchlik, A. Triska, Solid State Comm. **39,** 1199 (1981).
[8] M. Vanacek, J. Kocka, A. Poruba, A. Fejfar, J. Appl. Phys. **78**, 6203 (1995).
[9] C. R. Wronski, B. Abeles, T. Tiedje, G. Cody, Solid State Comm. **44,** 1423 (1982).
[10] D. Ritter, K. Weiser, Opt. Comm. **57**, 336 (1986).
[11] S. Wiedeman, M. S. Benett, J. L. Newton, Mater. Res. Soc. Proc. **95**, 145 (1987).
[12] I. Chen, L. Jiao, R. W. Collins, C. W. Wronski, J. Non-Cryst. Solids **198-200**, 391 (1996).
[13] D. R. Ritter, E. Zeldow, K. Weizer, J. Appl. Phys. **62,** 4563 (1987).
[14] M. Güneş, D. Akdaş, O. Göktaş, R. Carius, J. Klomfass, F. Finger, J. Mater. Sci: Mater. Electronics **14,** 729 (2003).
[15] R. Carius, Private Communication.
[16] F. Finger, S. Klein, T. Dylla, A.L. Baia Neto, O. Vetterl, R. Carius, Mater. Res. Soc. Symp. Proc. **175**, A.16.3.1 (2002)
[17] Y. Mai, S. Klein, X. Geng, F. Finger, Appl. Phys. Lett. (2004).
[18] A. Gross, O. Vetterl, A. Lambertz, F. Finger, H. Wagner, A. Dasgupta, Appl. Phys. Lett. **79**, 2841 (2001).
[19] S. Klein, F. Finger, R. Carius, B. Rech, L. Houben, M. Luysberg, M. Stutzmann, Mater. Res. Soc. Symp. Proc. **715,** A.26.2 (2002).